Unstable ice stream in Greenland during the Younger Dryas cold event

Vincent Rinterknecht, Vincent Jomelli, Daniel Brunstein, Vincent Favier, Valérie Masson-Delmotte, Didier Bourlès, Laëtitia Leanni, Romain Schläppy

^{10}Be dating

Samples from erratic crystalline boulders come from sites proximal to the Pjetursson's Moraine (n = 6) and from the top of the Pjetursson's Moraine (n = 1) (Fig. DR1). All samples were collected with a manual jackhammer to leave minimal visible impact. The crystalline lithology of the seven boulders is gneissic, which is a quartz-rich lithology suitable for surface exposure dating using cosmogenic ^{10}Be (Table DR1). We sampled erratic boulders ranging between 1 and 7 m^3 selecting the best candidates for surface exposure dating (Fig. DR2). Horizontal or near horizontal surfaces were sampled to avoid sample geometry corrections. Geographic positions and elevations were recorded with a handheld GPS. Shielding of all sampled surfaces by surrounding hills was recorded with a clinometer and compass. Samples were collected at elevations above the maximum local marine limit, which is 90 m in the southern and southeastern parts of Disko Island (Ingólfsson et al., 1990).

Samples were crushed and sieved. The 0.25 to 1 mm quartz fraction was decontaminated by successive acid leaching (HCl+H_2SiF_6 then dilute HF). Purified quartz was spiked with 100 µl of a 3025 ppm home-made carrier then dissolved in 48% HF. Beryllium was complexed by acetyl acetone in a 50% EDTA solution then extracted using solvent extraction. Beryllium hydroxides were dried and oxidized at 800°C to BeO. Beryllium oxide was mixed with 325 mesh niobium powder prior to measurement at ASTER, the French AMS located at CEREGE, Aix en Provence. Data were calibrated directly against the National Institute of Standards and Technology standard reference material 4325 by using an assigned ^{10}Be/^{9}Be ratio of $(2.79 \pm 0.03) \times 10^{-11}$ (Nishiizumi et al., 2007) and a ^{10}Be half-life of $(1.36 \pm 0.07) \times 10^6$ years (Chmeleff et al., 2010; Korschinek et al., 2010). Analytical uncertainties (reported as 1 sigma) include a conservative 0.5% uncertainty based on long-term measurements of standards, a 1 sigma statistical error on counted ^{10}Be events, and the uncertainty associated with the chemical and analytical blank correction (associated ^{10}Be/^{9}Be blank ratio was 9.5×10^{-16}).

In order to determine surface exposure ages from the ^{10}Be concentrations measured in the quartz fractions, we calculated the exposure ages using the CRONUS-Earth online calculator (Balco et al., 2008) and the calibration data set from Young et al. (2013b). The use of alternative local ^{10}Be production rates (Balco et al., 2009; Briner et al., 2012) does not significantly modify the exposure ages nor therefore our conclusions.

The production rates of cosmogenically produced isotopes such as ^{10}Be are affected by the altitude and latitude of the sample site, as well as the variation of the geomagnetic field at the sample location. The CRONUS-Earth online ^{10}Be exposure age calculator (http://hess.ess.washington.edu/math/) calculates surface exposure ages using four different

scaling schemes summarizing the main attempts to correct for these effects (Balco et al., 2008). The use of these alternative scaling schemes results in ^{10}Be age difference of < 2% and do not affect the overall ^{10}Be chronology for the region as all ages were calculated using the same scaling scheme.

We report here the exposure ages calculated with the "Lm" scaling scheme (Table DR1). The "Lm" method provides the closest fit to existing calibration data and uses the scaling factors proposed by (Lal, 1991) and (Stone, 2000), and is further accommodated for paleomagnetic corrections following the description of Nishiizumi (1989). As such, we think that the exposure ages calculated with this scaling method (Lm) represent the best age estimation of the samples' exposure. We interpret these exposure ages as minimum ages and use them as the basis for our discussion.

We correct the production rate for sample thickness using an exponential function (Lal, 1991) and assuming a density of 2.7 g cm^{-3} for gneiss. The production rates could be further affected by intermittent snow cover, vegetation cover, and erosion rate. We do not apply any corrections for snow cover as the sampling sites are located in an open and windswept area. Furthermore, no significant vegetation (e.g. forest) is present at these latitudes and thus no correction for vegetation cover was necessary. The surfaces of the sampled boulders show evidence of glacial polish, a sign that erosion was minimal if any, since deposition. The ^{10}Be ages are thus not corrected for erosion.

Because of the elevation dependence of the ^{10}Be production rate we must account for the elevation variation through time as a consequence of glacio-isostatic uplift and sea-level depression. Disko Island has been undergoing post-deglacial isostatic rebound, with modern lithosphere responses ranging from 90 m on the southern and southeastern coast to 60 m on the northwestern coast (Ingólfsson et al., 1990). We used the local sea level record of isostatic uplift (Ingólfsson et al., 1990) and far-field records of sea level rise (Bard et al., 1996; Bard et al., 1990; Fleming et al., 1998) to derive the integrated change in production rate experienced by our samples as a result of post-glacial uplift. We corrected for as much as 190 m of uplift in the sampling area and the production rate was lowered by as much a 5% (sample DIS-LM03).

A Shapiro-Wilk test indicates that we cannot reject the normality assumption (W = 0.94, p-value = 0.67) for the distribution of the seven exposure ages. Since the observed variability (7%) is less than our analytical uncertainties (average 9%, with a range between 6 and 14%), we report the error-weighted mean age and the error-weighted mean of the analytical uncertainty (3%): 12.2 ± 0.4 ^{10}Be ka. When including in quadrature the error associated with the ^{10}Be production rate, we calculate a moraine age of 12.2 ± 0.6 ^{10}Be ka.

Published ^{10}Be ages

We summarized the data set of ^{10}Be ages existing for the Disko Bugt area (Table DR3). All ages were recalculated using the same method and production rate (Baffin Bay: 3.96 ± 0.15 atoms g^{-1} a^{-1}) (Young et al., 2013b) including the samples from Kelley et al. (2013). However, some exposure ages do not take into account the post-glacial isostatic uplift effect on the production rate. This effect can introduce a 2 to 5% decrease of the production rate depending on the method used to account for the lithospheric rebound and sea level rise effect (Young et al., 2013a). The resultant exposure ages could thus be 2 to 5% older but the

difference does not affect the relative chronology and our interpretation of the deglaciation of Disko Bugt.

Published ^{14}C ages

Most radiocarbon ages were calibrated using the CALIB06 (http://calib.qub.ac.uk/calib/) (Stuiver et al., 2010) with the INTCAL09 calibration curve (Reimer et al., 2009). Some radiocarbon ages were calibrated using earlier versions of the CALIB program (see footnote Table DR2). All ages discussed in our paper were calibrated using CALIB06 and MARINE09 with a ΔR of 140 years.

Supplementary References

Balco, G., Briner, J., Finkel, R. C., Rayburn, J. A., Ridge, J. C., and Schaefer, J. M., 2009, Regional beryllium-10 production rate calibration for late-glacial northeastern North America: Quaternary Geochronology, v. 4, no. 2, p. 93-107.

Balco, G., Stone, J. O., Lifton, N. A., and Dunai, T. J., 2008, A complete and easily accessible means of calculating surface exposure ages or erosion rates from ^{10}Be and ^{26}Al measurements: Quaternary Geochronology, v. 3, p. 174-195.

Bard, E., Hamelin, B., Arnold, M., Montaggioni, L., Cabioch, G., Faure, G., and Rougerie, F., 1996, Deglacial sea-level record from Tahiti corals and the timing of global meltwater discharge: Nature, v. 382, p. 241-244.

Bard, E., Hamelin, B., and Fairbanks, R. G., 1990, U-Th ages obtained by mass spectrometry in corals from Barbados: sea level during the past 130000 years: Nature, v. 346, p. 456-458.

Bennike, O., 2000, Palaeoecological studies of Holocene lake sediments from west Greenland: Palaeogeography, Palaeoclimatology, Palaeoecology, v. 155, no. 3–4, p. 285-304.

Briner, J. P., Young, N. E., Goehring, B. M., and Schaefer, J. M., 2012, Constraining Holocene ^{10}Be production rates in Greenland: Journal of Quaternary Science, v. 27, no. 1, p. 2-6.

Chmeleff, J., von Blanckenburg, F., Kossert, K., and Jakob, D., 2010, Determination of the ^{10}Be half-life by multicollector ICP-MS and liquid scintillation counting: Nuclear Instruments and Methods in Physics Research Section B: Beam Interactions with Materials and Atoms, v. 268, no. 2, p. 192-199.

Corbett, L. B., Young, N. E., Bierman, P. R., Briner, J. P., Neumann, T. A., Rood, D. H., and Graly, J. A., 2011, Paired bedrock and boulder ^{10}Be concentrations resulting from early Holocene ice retreat near Jakobshavn Isfjord, western Greenland: Quaternary Science Reviews, v. 30, no. 13–14, p. 1739-1749.

Fleming, K., Johnston, P., Zwartz, D., Yokoyama, Y., Lambeck, K., and Chappell, J., 1998, Refining the eustatic sea-level curve since the Last Glacial Maximum using far- and intermediate-field sites: Earth and Planetary Science Letters, v. 163, p. 327-342.

Ingólfsson, O., Frich, P., Funder, S., and Humlum, O., 1990, Paleoclimatic implications of an early Holocene glacier advance on Disko Island, West Greenland: Boreas, v. 19, no. 4, p. 297-311.

Jennings, A. E., Walton, M. E., Ó Cofaigh, C., Kilfeather, A., Andrews, J. T., Ortiz, J. D., De Vernal, A., and Dowdeswell, J. A., 2014, Paleoenvironments during Younger Dryas-Early Holocene retreat of the Greenland Ice Sheet from outer Disko Trough, central west Greenland: Journal of Quaternary Science, v. 29, no. 1, p. 27-40.

Kelley, S. E., Briner, J. P., and Young, N. E., 2013, Rapid ice retreat in Disko Bugt supported by ^{10}Be dating of the last recession of the western Greenland Ice Sheet: Quaternary Science Reviews, v. 82, p. 13-22.

Korschinek, G., Bergmaier, A., Faestermann, T., Gerstmann, U. C., Knie, K., Rugel, G., Wallner, A., Dillmann, I., Dollinger, G., and von Gostomski, C. L., 2010, A new value for the half-life of ^{10}Be by Heavy-Ion Elastic Recoil Detection and liquid scintillation counting: Nuclear Instruments and Methods in Physics Research Section B: Beam Interactions with Materials and Atoms, v. 268, no. 2, p. 187-191.

Lal, D., 1991, Cosmic ray labeling of erosion surfaces: *in situ* nuclide production rates and erosion models: Earth and Planetary Science Letters, v. 104, p. 424-439.

Lloyd, J. M., Park, L. A., Kuijpers, A., and Moros, M., 2005, Early Holocene palaeoceanography and deglacial chronology of Disko Bugt, West Greenland: Quaternary Science Reviews, v. 24, no. 14–15, p. 1741-1755.

Long, A. J., and Roberts, D. H., 2002, A revised chronology for the 'Fjord Stade' moraine in Disko Bugt, west Greenland: Journal of Quaternary Science, v. 17, no. 5-6, p. 561-579.

Long, A. J., and Roberts, D. H., 2003, Late Weichselian deglacial history of Disko Bugt, West Greenland, and the dynamics of the Jakobshavns Isbrae ice stream: Boreas, v. 32, no. 1, p. 208-226.

Long, A. J., Roberts, D. H., and Wright, M. R., 1999, Isolation basin stratigraphy and Holocene relative sea-level change on Arveprinsen Ejland, Disko Bugt, West Greenland: Journal of Quaternary Science, v. 14, no. 4, p. 323-345.

McCarthy, D. J., 2011, Late Quaternary Ice-Ocean Interactions in Central West Greenland.: Durham, Available at Durham E-Theses Online p.

Nishiizumi, K., Imamura, M., Caffee, M. W., Southon, J. R., Finkel, R. C., and McAninch, J., 2007, Absolute Calibration of ^{10}Be AMS Standards: Nuclear Instruments and Methods in Physics Research B, v. 258, p. 403-413.

Nishiizumi, K., Winterer, E. L., Kohl, C. P., Klein, J., Middleton, R., Lal, D., and Arnold, J. R., 1989, Cosmic ray production rates of ^{10}Be and ^{26}Al in quartz from glacially polished rocks: Journal of Geophysical Research, v. 94, p. 17907-17915.

Ó Cofaigh, C., Dowdeswell, J. A., Jennings, A. E., Hogan, K. A., Kilfeather, A., Hiemstra, J. F., Noormets, R., Evans, J., McCarthy, D. J., Andrews, J. T., Lloyd, J. M., and Moros, M., 2013, An extensive and dynamic ice sheet on the West Greenland shelf during the last glacial cycle: Geology, v. 41, no. 2, p. 219-222.

Perner, K., Moros, M., Snowball, I. A. N., Lloyd, J. M., Kuijpers, A., and Richter, T., 2013, Establishment of modern circulation pattern at c. 6000 cal a BP in Disko Bugt, central West Greenland: opening of the Vaigat Strait: Journal of Quaternary Science, v. 28, no. 5, p. 480-489.

Reimer, P. J., Baillie, M. G. L., Bard, E., Bayliss, A., Beck, J. W., Blackwell, P. G., Bronk Ramsey, C., Buck, C. E., Burr, G. S., Edwards, R. L., Friedrich, M., Grootes, P. M., Guilderson, T. P., Hajdas, I., Heaton, T. J., Hogg, A. G., Hughen, K. A., Kaiser, K. F., Kromer, B., McCormac, F. G., Manning, S. W., Reimer, R. W., Richards, D. A., Southon, J. R., Talamo, S., Turney, C. S. M., van der Plicht, J., and Weyhenmeyer, C. E., 2009, IntCal09 and Marine09 Radiocarbon Age Calibration Curves, 0–50,000 Years cal BP: Radiocarbon, v. 51, p. 1111-1150.

Roberts, D. H., Rea, B. R., Lane, T. P., Schnabel, C., and Rodés, A., 2013, New constraints on Greenland ice sheet dynamics during the last glacial cycle: Evidence from the Uummannaq ice stream system: Journal of Geophysical Research: Earth Surface, v. 118, no. 2, p. 519-541.

Stone, J., 2000, Air pressure and cosmogenic isotope production: Journal of Geophysical Research, v. 105, no. b10, p. 23753-23759.

Stuiver, M., Reimer, P. J., and Reimer, R. W., 2010, CALIB 6.0 WWW program and documentation. Avaialble at http://calib.qub.ac.uk/calib/.

Van der Veen, C. J., 1999, Fundamentals of Glacier Dynamics, Rotterdam, Balkema, 462 p.:

Young, N. E., Briner, J. P., Axford, Y., Csatho, B., Babonis, G. S., Rood, D. H., and Finkel, R. C., 2011a, Response of a marine-terminating Greenland outlet glacier to abrupt cooling 8200 and 9300 years ago: Geophysical Research Letters, v. 38, no. 24, p. L24701.

Young, N. E., Briner, J. P., Rood, D. H., Finkel, R. C., Corbett, L. B., and Bierman, P. R., 2013a, Age of the Fjord Stade moraines in the Disko Bugt region, western Greenland, and the 9.3 and 8.2 ka cooling events: Quaternary Science Reviews, v. 60, no. 0, p. 76-90.

Young, N. E., Briner, J. P., Stewart, H. A. M., Axford, Y., Csatho, B., Rood, D. H., and Finkel, R. C., 2011b, Response of Jakobshavn Isbrae, Greenland, to Holocene climate change: Geology, v. 39, p. 131-134.

Young, N. E., Schaefer, J. M., Briner, J. P., and Goehring, B. M., 2013b, A ^{10}Be production-rate calibration for the Arctic: Journal of Quaternary Science, v. 28, no. 5, p. 515-526.

Table DR1: Pjetursson's Moraine ^{10}Be sample characteristics

Sample name	Latitude (DD)	Longitude (DD)	Elevation (m asl)	Thickness (cm)	Shielding correction	Quartz dissolved (g)	^{9}Be carrier added (mg)*	^{10}Be/^{9}Be †	^{10}Be/^{9}Be uncertainty §	^{10}Be ages (ka)#
DIS-GM01	69.2683	-53.4841	82	1.5	0.997	18.46	100	4.75E-14	6.69E-15	12.0 ± 1.7
DIS-GM02	69.2671	-53.4755	98	1.0	0.991	11.62	100	3.27E-14	3.08E-15	12.9 ± 1.2
DIS-GM03	69.2670	-53.4764	98	1.5	0.997	26.15	100	6.52E-14	4.87E-15	11.4 ± 0.9
DIS-GM04	69.2663	-53.4778	97	1.5	0.997	27.81	101	8.60E-14	1.18E-14	14.2 ± 1.9
DIS-GM05	69.2645	-53.4810	93	2.0	0.997	20.73	101	5.68E-14	3.51E-15	12.7 ± 0.8
DIS-GM06	69.2644	53.4853	74	1.5	0.997	15.58	101	4.13E-14	3.21E-15	12.5 ± 1.0
DIS-LM03	69.2736	-53.4754	132	1.0	0.996	14.95	101	4.11E-14	2.81E-15	12.1 ± 0.8

* All samples were spike with 3025 µg/g ^{9}Be carrier.

† All samples measured at the ASTER facility. AMS results are standardized to NIST_27900.

§ Analytical uncertainties (reported as 1σ) include a conservative 0.5% uncertainty based on long-term measurements of standards, a 1σ statistical error on counted ^{10}Be events, and the uncertainty associated with the chemical and analytical blank correction (the process blank ^{10}Be/^{9}Be value is 9.5×10^{-16}).

All ages calculated using the developmental version of the CRONUS-Earth online ^{10}Be exposure age calculator version 2.2-cal-dev for the NENA production rate (http://hess.ess.washington.edu/math/al_be_v22/Age_input_NENA_calib.html)
All ages calculated using a time-dependent production rate model scaled for sample site specific post-glacial uplift and according to the Lal (1991)/Stone (2000) scaling scheme (Lm).
A standard atmosphere was used. No erosion and no snow cover were accounted for. A rock density of 2.7 g cm-3 was used

Table DR2: List of ^{14}C dates available in the Disko Bugt area.

Sample ID	Latitude (DD)	Longitude (DD)	Age (14C yr BP)	Age (cal yr BP)	Site	Context	Reference
AA-37711	69.1833	-51.8167	9485±65	10370±130*	Central Disko Bugt		(Young et al., 2013a)
AA-38840	68.4500	-51.0167	8136±57	9134±69†	Qeqertarsuatsiaq, Disko Bugt	Bulk sediment	(Long and Roberts, 2003)
AA-38841	68.4333	-51.0333	9270±61	10454±106†	Qeqertarsuatsiaq, Disko Bugt	Bulk sediment	(Long and Roberts, 2003)
AA-38842	68.4333	-51.0500	9330±99	10640±200†	Qeqertarsuatsiaq, Disko Bugt	Bulk sediment	(Long and Roberts, 2003)
AA-38843	68.5333	-51.1500	6662±54	7539±54†	Umivik, Disko Bugt	Bulk sediment	(Long and Roberts, 2003)
AA-38844	68.5333	-51.1500	9185±62	10382±82†	Umivik, Disko Bugt	Bulk sediment	(Long and Roberts, 2003)
AA-39655	68.6167	-52.1000	9180±80	10390±170†	SE Disko Bugt	Basal sediment bulk	(Long and Roberts, 2003)
AA-39659	68.6667	-51.1167	8585±86	9610±180†	SE Disko Bugt	Basal sediment bulk	(Long and Roberts, 2002)
AA-39661	68.6333	-50.9667	7059±62	7875±125*	SE Disko Bugt	Basal sediment bulk	(Young et al., 2013a)
AA-39664	68.6333	-50.9667	7414±72	8210±165*	SE Disko Bugt	Basal sediment bulk	(Young et al., 2013a)
AA-39665	68.6333	-50.9667	7733±56	8505±95*	SE Disko Bugt	Sediment bulk	(Young et al., 2013a)
AA-89913	70.5665	-60.3075	13211±92	14880±250*	Uummannaq trough	Mixed benthic foraminifers	(Ó Cofaigh et al., 2013)
AAR-3496	70.4625	-54.0225	10160±75	11710±370†	Nussuaq	Algae	(Bennike, 2000)
AAR-5	69.2833	-53.4667	9650±125	10495±150*	Disko Island	Shells	(Young et al., 2013a)
AAR-6839	69.1702	-51.3952	7843±70	8320±135†	Central Disko Bugt	Bivalve	(Lloyd et al., 2005)
Beta-107879	69.7605	-51.2348	8820±100	9756±58§	Arveprinsen Ejland	Gytjja	(Long et al., 1999)
Beta-110748	69.7670	-51.2549	6290±40	7136±25§	Arveprinsen Ejland		(Long et al., 1999)
Beta-112543	69.7735	-51.2492	6950±150	7764±72§	Arveprinsen Ejland		(Long et al., 1999)
Beta-112544	69.7667	-51.2326	7780±120	8642±78§	Arveprinsen Ejland		(Long et al., 1999)
Beta-178165	69.1167	-50.6667	6760±40	7600±80*	Jakobshavn Isfjord	Basal sediment bulk	(Young et al., 2013a)
Beta-178168	69.1000	-50.6333	7960±40	8820±180*	Jakobshavn Isfjord	Basal sediment bulk	(Young et al., 2013a)
Beta-178169	69.1167	-50.6167	6750±40	7590±80*	Jakobshavn Isfjord	Basal sediment bulk	(Young et al., 2013a)
Beta-178170	69.1167	-50.5833	6910±40	7740±80*	Jakobshavn Isfjord	Basal sediment bulk	(Young et al., 2013a)
BETA-265212	67.9088	-58.7318	10620±60	11620±174*	Disko trough	Shell fragment	(Ó Cofaigh et al., 2013)
BETA-265217	68.2010	-57.7563	10910±60	12240±125*	Disko trough	Nuculana pernula	(Ó Cofaigh et al., 2013)
BETA-265221	67.5560	-59.8839	23310±160	27440±427*	Disko trough	Shell fragment	(Ó Cofaigh et al., 2013)
BETA-265222	67.7005	-59.3423	15380±70	18120±284*	Disko trough	Nuculana pernula	(Ó Cofaigh et al., 2013)

CURL-10090	69.3167	-50.1833	6290±15	7210±40*	Jakobshavn Isfjord	Basal sediment macrofossil	(Young et al., 2013a)
CURL-10441	69.2333	-50.0333	6360±25	7300±120*	Jakobshavn Isfjord	Basal sediment macrofossil	(Young et al., 2013a)
CURL-11061	69.1000	-51.0333	8180±25	9140±110*	Jakobshavn Isfjord	Plant macrofossils	(Young et al., 2013a)
CURL-11141	68.9667	-50.0667	7040±20	7520±55*	Jakobshavn Isfjord	Hiatella arctica	(Young et al., 2013a)
CURL-11374	69.1000	-51.0333	8210±20	9150±120*	Jakobshavn Isfjord	Plant macrofossils	(Young et al., 2013a)
CURL-11376	69.1000	-51.0333	8225±20	9190±100*	Jakobshavn Isfjord	Plant macrofossils	(Young et al., 2013a)
CURL-12594	69.1000	-51.0333	8245±20	9210±80*	Jakobshavn Isfjord	plant macrofossils	(Young et al., 2013a)
CURL-12603	69.2333	-50.0333	6185±15	7090±80*	Jakobshavn Isfjord		(Young et al., 2013a)
CURL-12693	68.6333	-50.9667	6975±25	7825±100*	SE Disko Bugt	Plant macrofossils	(Young et al., 2013a)
CURL-12698	68.6333	-50.9667	7030±25	7865±70*	SE Disko Bugt	Plant macrofossils	(Young et al., 2013a)
HEL-2210	69.3000	-53.2500	9060±120	10010±108§	Ippik	Shells	(Long et al., 1999)
HEL-362	68.6000	-53.5667	8970±170	9970±193§	Kannala	Shells	(Long et al., 1999)
Hel-369	68.6167	-50.8500	7210±170	8035±325*	SE Disko Bugt	Raised marine deposits	(Young et al., 2013a)
I-16390	70.2333	-54.7833	9200±150	10205±217*	Illorpaat	Shells	(Long et al., 1999)
I-16393	70.2667	-54.6167	9920±150	11010±346*	Niaqussat	Shells	(Long et al., 1999)
K-1818	69.0000	-51.0000	8630±130	9790±370*	Jakobshavn Isfjord	Raised marine deposits	(Young et al., 2013a)
K-2022	69.0500	-51.1333	7690±120	8800±340*	Jakobshavn Isfjord	Marine seds	(Young et al., 2013a)
K-2023	69.0167	-51.1333	8680±135	9820±340*	Jakobshavn Isfjord	Raised marine deposits	(Young et al., 2013a)
K-3660	69.6667	-52.0000	8700±120	9650±129§	Aqajarua	Shells	(Long et al., 1999)
K-3664	69.7333	-51.4000	8760±125	9757±131§	Appat	Shells	(Long et al., 1999)
K-3667	69.6667	-52.0167	8950±125	9960±157§	Aqajarua	Gytjja	(Long et al., 1999)
K-4567	69.3000	-53.2500	9220±130	10220±144§	Ippik	Shells	(Long et al., 1999)
K-5133	68.4333	-52.9500	11320±140	13230±159§	Qeqertarssuatsiaq	Gytjja	(Long et al., 1999)
K-5510	70.0500	-54.7500	9350±100	10330±189§	Inussuup Kua	Shells	(Long et al., 1999)
K-992	69.0333	-51.0167	7110±140	7930±270*	Jakobshavn Isfjord	marine seds	(Young et al., 2013a)
K-993	68.9333	-50.9667	7650±140	8570±400*	Jakobshavn Isfjord	marine seds	(Young et al., 2013a)
K-994	70.0667	-52.1000	8940±170	9950±198§	Saqqaq	Shells	(Long et al., 1999)
KIA-23028	69.4833	-50.7000	6810±40	7660±40*	Pekitsoq	Basal sediment bulk	(Young et al., 2013a)
LU-3037	70.1667	-54.8333	9360±140	10360±219§	Hammer Dal	Shells	(Long et al., 1999)
LU-3041	69.7333	-54.8333	9060±90	10010±97§	Ivisaarqut	Shells	(Long et al., 1999)

OS-85087	68.6167	-50.9500	7220±40	8060±100*	SE Disko Bugt	Plant macrofossils	(Young et al., 2013a)
AA84714	68.6092	-55.3265	10545±45	11480±65*	Egedesminde Dyb	Macoma calcarea	(Jennings et al., 2014)
RCD-21	68.9833	-53.3167	8690±90	9620±111§	Nunarssuaq	Shells	(Long et al., 1999)
Ua-1086	69.2000	-51.0667	8795±130	9470±350*	Jakobshavn Isfjord	Raised marine deposits	(Young et al., 2011b)
UA-1789	70.3833	-54.9500	10470±130	12390±190§	Talerua	Shells	(Long et al., 1999)
Ua-4573	68.9333	-50.8833	8215±80	8750±220*	Jakobshavn Isfjord	Marine seds	(Young et al., 2013a)
Ua-4574	69.0000	-50.9667	9180±75	9950±230*	Jakobshavn Isfjord	Raised marine deposits	(Young et al., 2013a)
Ua-4575	69.0333	-50.9333	8140±95	8670±260*	Jakobshavn Isfjord	Marine seds	(Young et al., 2013a)
Poz-30991	68.3973	-55.1297	10840±60	12072±133*	Jakobshavn Isfjord	Mollusc (Portlandia arctica)	(McCarthy, 2011)
LuS 9708	68.4719	-54.0020	9455±90	10130±131*	Jakobshavn Isfjord	Mix benthic foraminifera	(Perner et al., 2013)
LuS 9921	68.9679	-53.1851	8085±80	8417.5±89*	Egedesminde Dyb	Mix benthic foraminifera	(Perner et al., 2013)
AA82363	70.2196	-53.0532	2352±37	1807±44*	Vaigat Strait	Turitella polaris	(Perner et al., 2013)
LuS 8547	70.8159	-56.8483	8340±70	8714±127*	Uummannaq Trough	Mix benthic foraminifera	(Perner et al., 2013)

* Calibrated using CALIB06 and INTCAL09 or MARINE09
† Calibrated using CALIB04
§ Calibrated using CALIB03

Table DR3: List of available ^{10}Be dates in the Disko Bugt area

Sample name	Latitude (DD)	Longitude (DD)	Elevation (m)	Thickness (cm)	Density (g cm^{-3})	Shielding correction	[Be-10] (atoms g^{-1})	Error in [Be-10] (atoms g^{-1})	Name of Be-10 standardization	Be-10 age (ka)†	Reference
DISKO-01	69.2624	-53.5521	150*	3.0	2.65	0.992	4.84E+04	9.12E+02	07KNSTD	9.9 ± 0.2	(Kelley et al.,2013)
DISKO-02	69.2621	-53.5508	153*	3.0	2.65	0.992	4.92E+04	9.47E+02	07KNSTD	10.0 ± 0.2	(Kelley et al.,2013)
DISKO-03	69.2637	-53.5548	173*	3.0	2.65	0.992	4.32E+04	8.30E+02	07KNSTD	8.6 ± 0.2	(Kelley et al.,2013)
KE-11-01	68.9845	-53.3337	89*	3.0	2.65	1.000	5.36E+04	2.89E+03	07KNSTD	11.6 ± 0.6	(Kelley et al.,2013)
KE-11-02	68.9843	-53.3337	87*	1.0	2.65	1.000	5.00E+04	1.04E+03	07KNSTD	10.7 ± 0.2	(Kelley et al.,2013)
QA-11-05	68.8473	-51.1676	195*	2.5	2.65	1.000	5.08E+04	2.30E+03	07KNSTD	9.8 ± 0.4	(Kelley et al.,2013)
QA-11-02	68.8106	-51.1400	420*	3.0	2.65	1.000	6.75E+04	1.23E+03	07KNSTD	10.4 ± 0.2	(Kelley et al.,2013)
QA-11-01	68.8046	-51.1552	360*	3.0	2.65	1.000	6.47E+04	1.55E+03	07KNSTD	10.6 ± 0.3	(Kelley et al.,2013)
SN-11-07	68.6931	-52.6969	119*	1.5	2.65	1.000	5.34E+04	1.01E+03	07KNSTD	11.1 ± 0.2	(Kelley et al.,2013)
SN-11-02	68.6725	-52.7072	119*	2.0	2.65	1.000	5.26E+04	9.93E+02	07KNSTD	10.9 ± 0.2	(Kelley et al.,2013)
SN-11-04	68.6491	-52.6664	220*	3.0	2.65	1.000	5.64E+04	1.35E+03	07KNSTD	10.6 ± 0.3	(Kelley et al.,2013)
SN-11-05	68.6491	-52.6649	221*	2.0	2.65	1.000	5.50E+04	1.29E+03	07KNSTD	10.3 ± 0.2	(Kelley et al.,2013)
JAKN08-01	69.2055	-51.1244	96	2.5	2.65	1.000	4.76E+04	1.17E+03	07KNSTD	10.2 ± 0.3	(Young et al., 2011a; 2011b)
JAKN08-08	69.1993	-50.9674	322	1.0	2.65	1.000	6.14E+04	1.73E+03	07KNSTD	10.3 ± 0.3	(Young et al., 2011a; 2011b)
JAKN08-21	69.2432	-50.9807	374	1.0	2.65	1.000	6.39E+04	3.38E+03	07KNSTD	10.2 ± 0.5	(Young et al., 2011a; 2011b)
JAKN08-22	69.2410	-50.9614	344	4.5	2.65	1.000	5.96E+04	1.87E+03	07KNSTD	10.1 ± 0.3	(Young et al., 2011a; 2011b)
09GRO-01	69.1098	-51.0415	188	5.0	2.65	1.000	5.02E+04	1.25E+03	07KNSTD	10.0 ± 0.2	(Young et al., 2011a; 2011b)
JAKN08-13	69.1844	-50.9060	175	2.5	2.65	1.000	4.11E+04	1.04E+03	07KNSTD	8.1 ± 0.2	(Young et al., 2011a; 2011b)
FST08-BR	69.1974	-51.0541	60	2.0	2.65	0.999	5.38E+04	1.34E+03	07KNSTD	12.0 ± 0.3	(Young et al., 2011a; 2011b)
FST08-04	69.1465	-51.0538	60	2.0	2.65	0.999	3.63E+04	9.41E+02	07KNSTD	8.1 ± 0.2	(Young et al., 2011a; 2011b)
09GRO-03	69.1137	-51.0643	119	3.0	2.65	1.000	3.89E+04	1.14E+03	07KNSTD	8.2 ± 0.2	(Young et al., 2011a; 2011b)
09GRO-06	69.1162	-50.9911	240	4.5	2.65	1.000	4.15E+04	1.32E+03	07KNSTD	7.8 ± 0.2	(Young et al., 2011a; 2011b)
09GRO-33	69.1912	-51.0074	120	4.5	2.65	1.000	3.75E+04	1.17E+03	07KNSTD	8.0 ± 0.2	(Young et al., 2011a; 2011b)
JAKN08-28	69.2407	-49.9852	215	1.0	2.65	1.000	3.96E+04	1.90E+03	07KNSTD	7.4 ± 0.4	(Young et al., 2011a)

JAKN08-39	69.2214	-49.9952	206	3.0	2.65	1.000	3.87E+04	1.26E+03	07KNSTD	7.4 ± 0.2	(Young et al., 2011a)
JAKN08-40	69.2256	-50.0569	147	2.0	2.65	1.000	3.89E+04	9.97E+02	07KNSTD	7.9 ± 0.2	(Young et al., 2011a)
JAKN08-44	69.3078	-50.1479	347	2.0	2.65	1.000	4.45E+04	1.68E+03	07KNSTD	7.3 ± 0.3	(Young et al., 2011a)
JAKN08-56	69.3005	-50.3287	425	1.0	2.65	1.000	4.94E+04	1.21E+03	07KNSTD	7.5 ± 0.2	(Young et al., 2011a)
JAKS08-33	69.1471	-50.1245	222	1.0	2.65	1.000	4.07E+04	1.73E+03	07KNSTD	7.6 ± 0.3	(Young et al., 2011a)
JAKS08-34	69.1465	-50.1037	180	2.0	2.65	1.000	3.80E+04	9.75E+02	07KNSTD	7.4 ± 0.2	(Young et al., 2011a)
09GRO-08	69.1131	-51.0371	170	1.0	2.65	1.000	4.21E+04	1.04E+03	07KNSTD	8.2 ± 0.2	(Young et al., 2011b)
09GRO-09	69.1130	-51.0360	170	1.0	2.65	1.000	4.23E+04	8.00E+02	07KNSTD	8.3 ± 0.2	(Young et al., 2011b)
09GRO-11	69.1129	-51.0344	170	4.0	2.65	1.000	4.05E+04	9.37E+02	07KNSTD	8.1 ± 0.2	(Young et al., 2011b)
09GRO-12	69.1130	-51.0343	170	3.0	2.65	1.000	4.17E+04	9.63E+02	07KNSTD	8.3 ± 0.2	(Young et al., 2011b)
09GRO-24	69.2476	-50.7697	300	2.0	2.65	1.000	5.15E+04	9.69E+02	07KNSTD	8.9 ± 0.2	(Young et al., 2011b)
09GRO-27	69.2372	-50.8373	280	5.0	2.65	1.000	5.03E+04	9.70E+02	07KNSTD	9.1 ± 0.2	(Young et al., 2011b)
FST08-01	69.2022	-51.0878	75	1.0	2.65	0.999	3.89E+04	6.62E+02	07KNSTD	8.4 ± 0.1	(Young et al., 2011b)
FST08-02	69.2019	-51.0860	75	1.0	2.65	0.999	3.69E+04	7.38E+02	07KNSTD	8.0 ± 0.2	(Young et al., 2011b)
10GRO-08	68.6695	-50.9987	119	3.5	2.65	1.000	4.46E+04	8.53E+02	07KNSTD	9.4 ± 0.2	(Young et al., 2013)
10GRO-18	68.6164	-51.0512	164	4.5	2.65	1.000	4.62E+04	1.14E+03	07KNSTD	9.3 ± 0.2	(Young et al., 2013)
10GRO-33	68.7027	-50.8445	312	3.0	2.65	0.998	5.40E+04	1.01E+03	07KNSTD	9.3 ± 0.2	(Young et al., 2013)
10GRO-34	68.7000	-50.8209	332	2.0	2.65	1.000	5.67E+04	1.06E+03	07KNSTD	9.5 ± 0.2	(Young et al., 2013)
10GRO-01	68.6356	-50.9715	105	3.5	2.65	1.000	4.26E+04	8.60E+02	07KNSTD	9.1 ± 0.2	(Young et al., 2013)
10GRO-10	68.6216	-50.9427	145	4.0	2.65	0.997	4.15E+04	1.03E+03	07KNSTD	8.6 ± 0.2	(Young et al., 2013)
10GRO-11	68.6216	-50.9423	145	3.0	2.65	0.997	4.09E+04	1.37E+03	07KNSTD	8.4 ± 0.3	(Young et al., 2013)
10GRO-25	68.6142	-51.0298	166	2.0	2.65	1.000	4.53E+04	8.78E+02	07KNSTD	9.0 ± 0.2	(Young et al., 2013)
10GRO-31	68.7090	-50.8077	132	1.0	2.65	0.987	4.31E+04	8.14E+02	07KNSTD	8.9 ± 0.2	(Young et al., 2013)
10GRO-32	68.7135	-50.8439	85	2.0	2.65	0.989	4.15E+04	9.97E+02	07KNSTD	9.1 ± 0.2	(Young et al., 2013)
10GRO-07	68.6587	-50.9798	60	1.5	2.65	1.000	3.75E+04	7.52E+02	07KNSTD	8.3 ± 0.2	(Young et al., 2013)
10GRO-12	68.6219	-50.9385	140	1.5	2.65	1.000	4.00E+04	7.97E+02	07KNSTD	8.1 ± 0.2	(Young et al., 2013)
10GRO-13	68.6149	-50.9096	144	2.5	2.65	0.994	3.86E+04	1.25E+03	07KNSTD	7.9 ± 0.3	(Young et al., 2013)
10GRO-14	68.6153	-50.9027	132	2.0	2.65	0.997	4.00E+04	8.77E+02	07KNSTD	8.2 ± 0.2	(Young et al., 2013)

10GRO-28	68.7253	-50.6822	246	3.0	2.65	0.999	4.06E+04	8.04E+02	07KNSTD	7.5 ± 0.1	(Young et al., 2013)
10GRO-35	68.7188	-50.5620	198	2.5	2.65	0.995	3.51E+04	9.95E+02	07KNSTD	6.8 ± 0.2	(Young et al., 2013)
10GRO-39	68.7104	-50.4712	206	1.5	2.65	1.000	3.85E+04	8.02E+02	07KNSTD	7.3 ± 0.2	(Young et al., 2013)
JAKS08-08	69.0627	-49.8804	371	2.0	2.65	1.000	4.03E+04	1.02E+03	07KNSTD	6.5 ± 0.2	(Young et al., 2013)
JAKS08-24	69.0694	-50.1478	314	3.0	2.65	1.000	4.43E+04	1.98E+03	07KNSTD	7.6 ± 0.3	(Young et al., 2013)
10GRO-40	68.7026	-50.4267	230	1.0	2.65	1.000	3.79E+04	9.20E+02	07KNSTD	7.0 ± 0.2	(Young et al., 2013)
10GRO-41	68.7030	-50.4288	230	1.5	2.65	1.000	3.80E+04	8.97E+02	07KNSTD	7.0 ± 0.2	(Young et al., 2013)
GL022	69.432	-50.289	515*	5.0	2.7	1.000	5.54E+04	1.03E+03	07KNSTD	8.0 ± 0.1	(Corbett et al., 2011)
GL023	69.433	-50.289	511*	3.0	2.7	1.000	5.35E+04	1.18E+03	07KNSTD	7.6 ± 0.2	(Corbett et al., 2011)
GL001	69.433	-50.272	434*	1.0	2.7	1.000	4.62E+04	1.34E+03	07KNSTD	6.9 ± 0.2	(Corbett et al., 2011)
GL002	69.433	-50.273	432*	2.0	2.7	1.000	4.86E+04	1.14E+03	07KNSTD	7.4 ± 0.2	(Corbett et al., 2011)
GL003	69.434	-50.266	395*	3.0	2.7	1.000	4.73E+04	1.19E+03	07KNSTD	7.5 ± 0.2	(Corbett et al., 2011)
GL004	69.434	-50.266	392*	2.0	2.7	1.000	4.99E+04	1.19E+03	07KNSTD	7.9 ± 0.2	(Corbett et al., 2011)
GL080	69.395	-50.416	621*	3.0	2.7	1.000	6.18E+04	1.38E+03	07KNSTD	7.9 ± 0.2	(Corbett et al., 2011)
GL081	69.395	-50.416	618*	1.5	2.7	1.000	6.01E+04	1.13E+03	07KNSTD	7.6 ± 0.1	(Corbett et al., 2011)
GL086	69.374	-50.458	304*	2.5	2.7	1.000	4.28E+04	1.10E+03	07KNSTD	7.4 ± 0.2	(Corbett et al., 2011)
GL087	69.374	-50.458	303*	2.0	2.7	1.000	4.45E+04	9.59E+02	07KNSTD	7.7 ± 0.2	(Corbett et al., 2011)
GL088	69.344	-50.429	95*	2.5	2.7	1.000	3.49E+04	8.37E+02	07KNSTD	7.5 ± 0.2	(Corbett et al., 2011)
GL089	69.344	-50.429	93*	2.5	2.7	1.000	3.61E+04	8.09E+02	07KNSTD	7.8 ± 0.2	(Corbett et al., 2011)
GL103	69.318	-50.640	578*	1.0	2.7	1.000	6.89E+04	1.72E+03	07KNSTD	9.0 ± 0.2	(Corbett et al., 2011)
GL104	69.318	-50.640	578*	5.0	2.7	1.000	6.26E+04	1.20E+03	07KNSTD	8.5 ± 0.2	(Corbett et al., 2011)
GL105	69.293	-50.602	300*	1.0	2.7	1.000	4.65E+04	1.07E+03	07KNSTD	8.0 ± 0.2	(Corbett et al., 2011)
GL106	69.293	-50.602	300*	2.0	2.7	1.000	4.58E+04	9.46E+02	07KNSTD	7.9 ± 0.2	(Corbett et al., 2011)
GL090	69.269	-50.581	93*	2.0	2.7	1.000	4.02E+04	8.42E+02	07KNSTD	8.6 ± 0.2	(Corbett et al., 2011)
GL091	69.269	-50.582	91*	2.0	2.7	1.000	3.61E+04	9.97E+02	07KNSTD	7.8 ± 0.2	(Corbett et al., 2011)
GL096	69.250	-50.823	468*	3.0	2.7	1.000	7.27E+04	1.40E+03	07KNSTD	10.8 ± 0.2	(Corbett et al., 2011)
GL097	69.251	-50.822	470*	2.0	2.7	1.000	6.62E+04	1.72E+03	07KNSTD	9.7 ± 0.3	(Corbett et al., 2011)
GL094	69.229	-50.810	308*	1.0	2.7	1.000	5.49E+04	1.44E+03	07KNSTD	9.3 ± 0.3	(Corbett et al., 2011)

GL095	69.229	-50.810	308*	2.5	2.7	1.000	4.61E+04	1.29E+03	07KNSTD	7.9 ± 0.2	(Corbett et al., 2011)
GL098	69.199	-50.791	163*	3.0	2.7	1.000	4.97E+04	1.07E+03	07KNSTD	10.0 ± 0.2	(Corbett et al., 2011)
GL092	69.230	-50.902	397*	1.0	2.7	1.000	6.59E+04	1.31E+03	07KNSTD	10.3 ± 0.2	(Corbett et al., 2011)
GL093	69.230	-50.902	397*	2.0	2.7	1.000	6.69E+04	1.68E+03	07KNSTD	10.5 ± 0.3	(Corbett et al., 2011)
GL100	69.227	-50.930	292*	2.0	2.7	1.000	5.95E+04	1.30E+03	07KNSTD	10.4 ± 0.3	(Corbett et al., 2011)
GL101	69.227	-50.929	295*	3.5	2.7	1.000	5.62E+04	1.06E+03	07KNSTD	9.9 ± 0.2	(Corbett et al., 2011)
GL107	69.180	-50.891	53*	1.0	2.7	1.000	3.66E+04	8.09E+02	07KNSTD	8.1 ± 0.2	(Corbett et al., 2011)
GL108	69.180	-50.891	53*	1.0	2.7	1.000	3.73E+04	1.03E+03	07KNSTD	8.3 ± 0.2	(Corbett et al., 2011)
GL102	69.207	-51.134	85*	1.0	2.7	1.000	4.79E+04	1.07E+03	07KNSTD	10.3 ± 0.2	(Corbett et al., 2011)

* The sample elevation was corrected for isostatic uplift. No star corresponds to no correction for the isostatic uplift.
† All ages calculated using the developmental version of the CRONUS-Earth online calculator (Balco et al., 2008) and a locally derived ^{10}Be production rate for Baffin Bay (Young et al., 2013b).

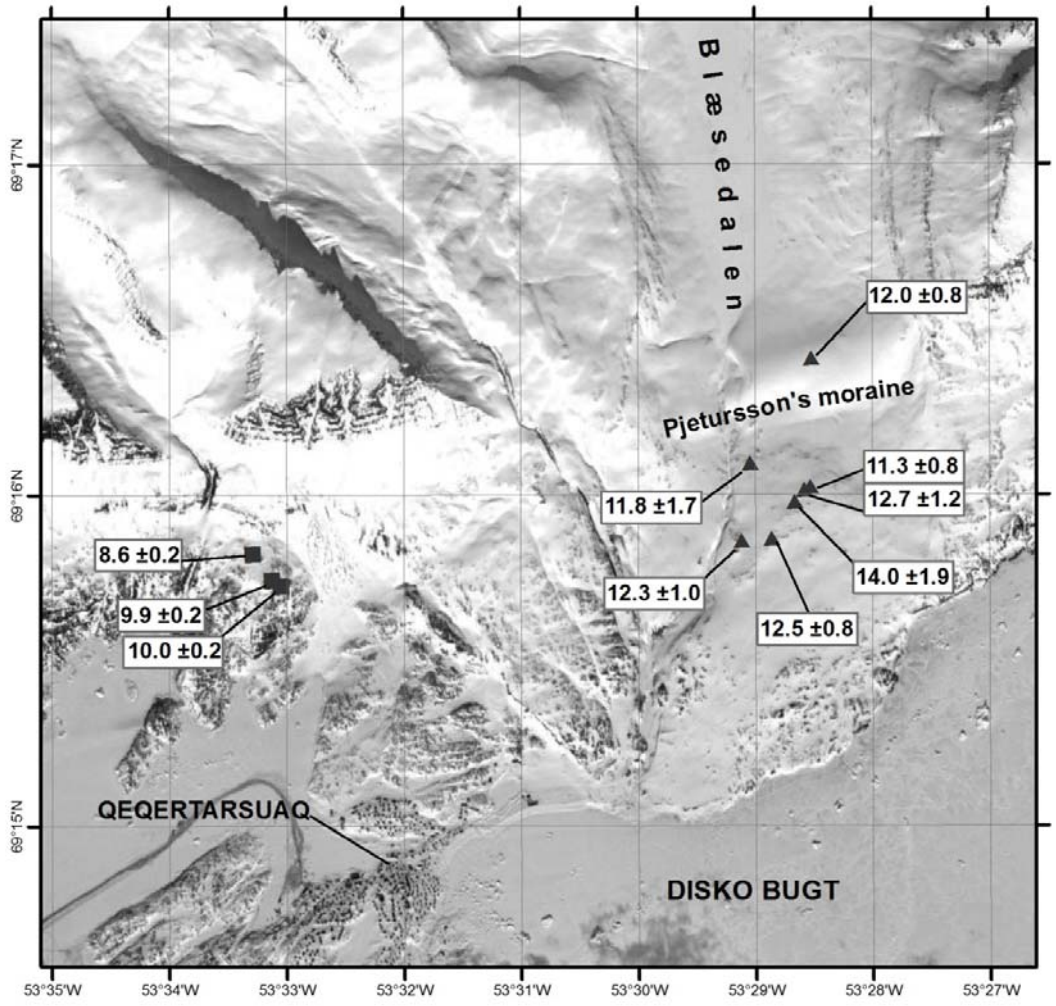

Figure DR1. Positions and surface exposure ages (in ka) of the boulder samples on the Pjetersson's Moraine and directly inboard the moraine (black triangles, this study), and positions of two bedrock and one boulder samples near Qeqertarsuaq (black squares, Kelley et al., 2013). Background image from Google Earth (accessed 23-09-2013).

Figure DR2. A. Erratic boulder sampled on the Pjetursson's Moraine. B. Erratic boulder sampled inboard the Pjetursson's Moraine, directly on top of the volcanic bedrock (in the background).

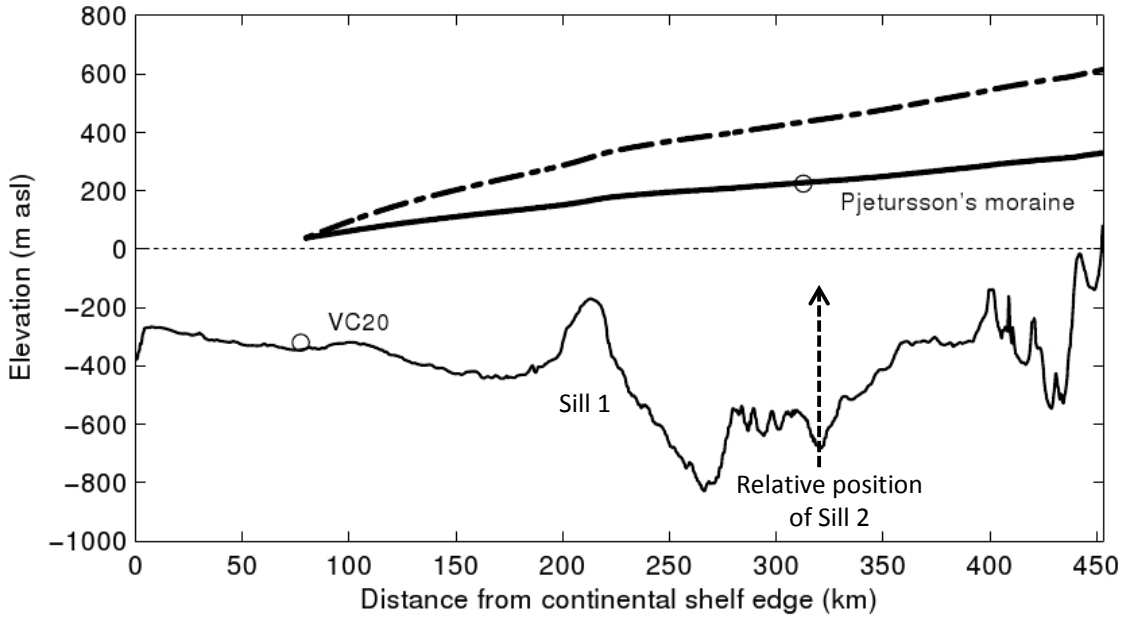

Figure DR3. Glacier surface elevations at 12.2 ± 0.6 ka based on Van der Veen (1999) model. The grounding line position is constrained by the presence of a till in core VC20 (O'Cofaigh et al., 2013). This position corresponds to a conservative approach because additional radiocarbon ages ~12 ka suggest that ice extended up to the continental shelf edge and slope. At the level of the grounding line the glacier elevation results from a simple hydrostatic equilibrium calculation. Two sliding conditions were tested: the basal shear stress values of 35 kPa (thick dashed line) and of 4 kPa (thick solid line), which are typical and minimum sliding conditions observed offshore for several neighbouring glaciers at the Last Glacial Maximum by Roberts et al. (2013). The low shear stress value resulted in a low profile ice stream (confined to the glacial trough) and ice shelf spreading in an open bay. Such a low shear stress value is supported by the location of the till and the Pjetursson's Moraine (distant by 200 km) as well their similar time of deposition: 12.2 ka.
The thin black line corresponds to the bed rock elevation assuming the mean sea level rise since 12.2 ka.